



1    **Robust multi-objective optimization under multiple-**  
2    **uncertainties using CM-ROPAR approach: case study of**  
3    **the water resources allocation in the Huaihe River Basin**

4  
5    Jitao Zhang<sup>1,2,3</sup>, Dimitri Solomatine<sup>2,3,4</sup>, Zengchuan Dong<sup>1</sup>

6    <sup>1</sup>College of Hydrology and water resources, Hohai University; Nanjing, 210000, China.

7    <sup>2</sup>Water Resources Section, Delft University of Technology; Delft, 2628 CD, Netherlands.

8    <sup>3</sup>IHE Delft Institute for Water Education; Delft, 2628 AX, Netherlands

9    <sup>4</sup>Water Problems Institute of RAS, Moscow 119333, Russia

10    *Correspondence to:* Zengchuan Dong (zcdong@hhu.edu.cn)

11    **Abstract.** Water resources managers need to make decisions in a constantly changing environment  
12    because the data relating to water resources is uncertain and imprecise. The Robust Optimization and  
13    Probabilistic Analysis of Robustness (ROPAR) algorithm is a well-suited tool for dealing with  
14    uncertainty. Still, the failure to consider multiple uncertainties and multi-objective robustness hinder the  
15    application of the ROPAR algorithm to practical problems. This paper proposes a robust optimization  
16    and robustness probabilistic analysis method that considers numerous uncertainties and multi-objective  
17    robustness for robust water resources allocation under uncertainty. The Copula function is introduced for  
18    analyzing the probabilities of different scenarios. The robustness with respect to the two objective  
19    functions is analyzed separately, and the Pareto frontier of robustness is generated. The relationship  
20    between the robustness with respect to the two objective functions is used to evaluate water resources  
21    management strategies. Use of the method is illustrated on a case study of water resources allocation in  
22    the Huaihe River Basin. The results demonstrate that the method opens a possibility for water managers  
23    to make more informed uncertainty-aware decisions.

24    1. Introduction

25    Water resources is a natural resource necessary for human survival (Chen et al., 2017) but also a driving  
26    force for social and economic development (Dong and Xu, 2019). Due to the increasing population and  
27    rapid growth of economy, a contradiction between the supply and demand of water resources is becoming  
28    more acute, water quality problems are becoming more prominent, and water resources have gradually  
29    become a bottleneck for socio-economic development (Zhuang et al., 2018). This phenomenon is  
30    particularly evident in rapidly urbanizing and vital agricultural and industrial production watersheds  
31    (Yang et al., 2017). In this category of watersheds, agricultural and industrial production pose a massive  
32    challenge to water resource management (WRM) due to accelerated urbanization and rapid socio-  
33    economic development (Sun et al., 2019). River basin managers must consider water sources in an  
34    integrated manner and decide how to allocate water resources between different water-using sectors and  
35    cities within the basin (Xiong et al., 2020).

36    Multi-objective optimization (MOO) is an effective method for improving water resources allocation



37 (WRA) schemes (Lu et al., 2017; Abdulbaki et al., 2017). MOO can provide decision-makers with WRA  
38 options based on their preferences for objectives, which makes it a well-suited decision-making method  
39 for WRM. Ashofteh et al. (2013) constructed a bottom-line-based multi-objective optimization model to  
40 calculate WRA schemes. Habibi Davijani et al. (2016) presented a multi-objective optimal allocation  
41 model of water resources in arid areas based on maximum socioeconomic benefits. However, WRM is  
42 not only a multi-stage and multi-objective problem but also a complex problem involving uncertainties  
43 and risk management (Yu and Lu, 2018). WRM departments often need to face decision challenges under  
44 uncertain conditions (Hassanzadeh et al., 2016; Ren et al., 2019). Climate change and human activities  
45 have led to an increase in uncertainties in rainfall and water demand in the basin and hence to uncertainty  
46 in managing water resource systems (Jin et al., 2020; Ma et al., 2020; Zhu et al., 2019). Uncertain factors  
47 may lead to the risk of water shortage in the basin, so the existing WRA schemes may not be longer  
48 applicable (Keath and Brown, 2009). Therefore, it is important to study WRA under uncertainty.

49 Previously, several methods were introduced to analyze uncertainty in WRM. Scenario building and  
50 analysis is regarded as an effective method for considering possible future events and analyzing future  
51 uncertainties (Zeng et al., 2019). The fuzzy logic theory is one of the methods to deal with uncertainty,  
52 which describes uncertainty by fuzzifying the decision variables (Nikoo et al., 2013). Two-stage  
53 stochastic programming (TSP) is also an available planning method in optimization under uncertainty  
54 (Li et al., 2020). However, these approaches do not explicitly evaluate the robustness of the WRA options,  
55 although they take into account the uncertainties in WRA.

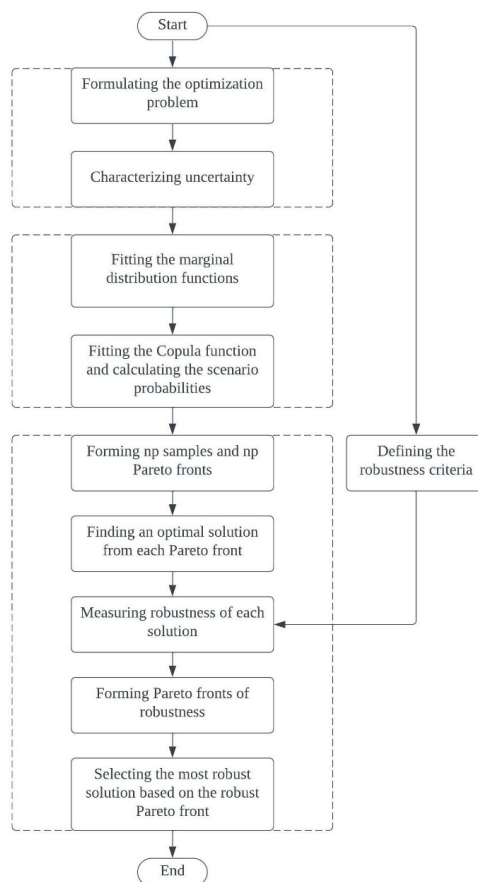
56 Robust multi-objective optimization (RMOO) is an effective method for forming robust WRA schemes.  
57 In relation to water, RMOO was actively applied in the field of water supply system (Kapelan et al., 2005;  
58 Kapelan et al., 2006). In the last decade, RMOO has been gradually applied to other areas of WRM.  
59 Yazdi et al. (2015) and Kang and Lansey (2013) applied robust optimization to design wastewater pipes  
60 by considering uncertainties such as climate change, urbanization, and population change. Marchi et al.  
61 (2016) formed stormwater harvesting schemes under variable climate conditions using RMOO. It should  
62 be pointed out however, that in the mentioned approaches the robustness is often “hidden” into the  
63 objective function or constraints and then a common MOO problem is solved that forms a single Pareto  
64 front. This is indeed an effective method to create solution set which in a certain sense is robust. However,  
65 this approach does not explicitly show the relationship between the solution and the uncertainty variables,  
66 which prevents the decision-maker from clearly understanding the impact of uncertainty, which can  
67 influence the decision. To answer this limitation, the procedure “Robust Optimization and Probabilistic  
68 Analysis of Robustness” (ROPAR) has been developed and presented first in (Solomatine, 2012). The  
69 method will generate multiple Pareto fronts, each corresponding to a sample of uncertain variables so  
70 that the statistical characteristics of the uncertainty of the solution can be analyzed. The ROPAR has been  
71 applied in the design of urban stormwater drainage pipes (Solomatine and Marquez-Calvo, 2019) and for  
72 water quality management in water distribution (Marquez Calvo et al., 2019; Quintiliani et al., 2019).

73 To the best of our knowledge, the presented versions of the ROPAR methodology have the following  
74 limitations:

- 75 ● ROPAR method has not been applied to the field of WRA.
- 76 ● ROPAR method only considers the single source of uncertainty: if there are two sources, then  
77 the joint probability of these sources needs to be considered.
- 78 ● ROPAR method only analyses the variability of one objective under conditions where the  
79 other objective function level is fixed. Although the ROPAR method can provide decision-  
80 makers with a robust solution under certain conditions, it does not take into account the



81 relationship between the two objective functions.  
82 Based on the above analysis, although the ROPAR method has proven to be suitable for dealing with  
83 uncertainty, it still needs improvement.  
84 In this study, we propose a Copula-Multi-objective Robust Optimization and Probabilistic Analysis of  
85 Robustness (CM-ROPAR) procedure under multiple uncertainties for WRA. The proposed new  
86 procedure of the ROPAR-family considers the joint probability distribution of uncertainties (in this case,  
87 inflows) and enables decision-makers to check the robustness of the two objective functions separately.  
88 The following text is structured as follows.  
89 First, the definition of robustness is presented. Then, the water demand and inflow in the study area was  
90 analyzed. Then, the steps of the CM- ROPAR algorithm and the water resources allocation model are  
91 described in detail. In addition, robustness criteria are chosen to analyze the robustness of the two  
92 objective functions separately. Finally, the applicability of the CM-ROPAR procedure is illustrated on a  
93 case study of the Huaihe River Basin (HRB).

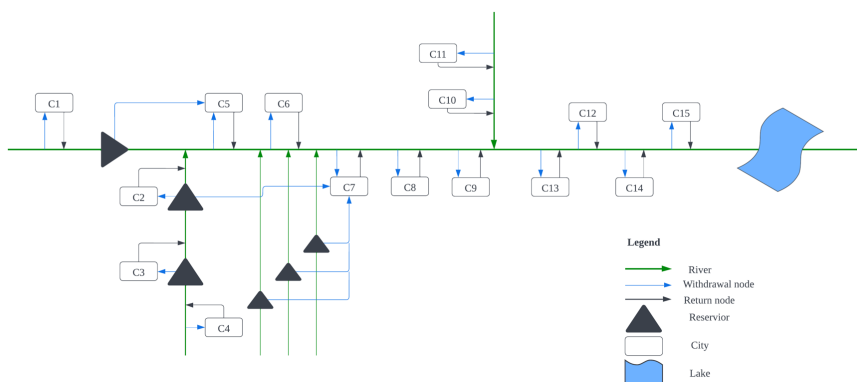


94  
95 **Figure 1.** Flowchart of CM-ROPAR.

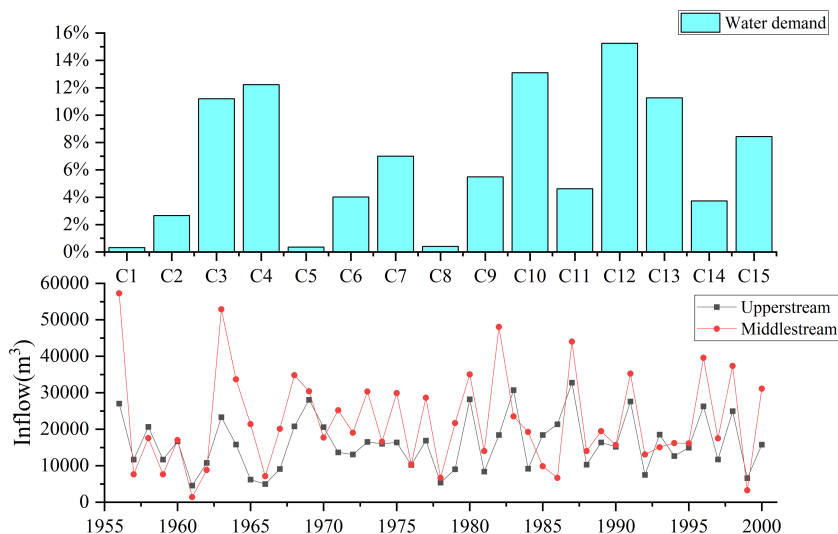
96 2. Case Study



97 The HRB is located in the eastern part of China, and as shown in Figure 2, the middle and upper basin  
 98 flows through 15 cities of Henan Province and Anhui Province. It is an important agricultural and  
 99 industrial production base in China (Xu et al., 2019). As shown in the Figure 3, the inflow of the HRB  
 100 varies significantly between different years and between different regions, and the water demand is  
 101 uneven among cities. In addition, due to the discharge of pollutants, the contradiction between supply  
 102 and demand of water resources in the middle and upper reaches of the HRB has become increasingly  
 103 fierce. Therefore, it is meaningful to study the optimal allocation of water resources and propose a robust  
 104 water resources allocation scheme based on the wet-dry encounters in the HRB.



105  
 106 **Figure 2.** Overview of watershed water supply.



107  
 108 **Figure 3.** Water demand proportion and inflow historical data.

109 3. Methodology



### 110 3.1 Method of Copula Function

111 Sklar proposed Copula theory in 1959, in which he decomposed an N-dimensional Joint Distribution  
112 Function (JDF) into a Copula function and N Marginal Distribution Functions (MDF), which are not  
113 required to be the same distribution for N variables and can be used to describe the correlation between  
114 arbitrary variables. Nelsen gave a strict definition of Copula function in 1999 (Nelsen et al., 2008).  
115 Copula function is the function that connects the JDF with their respective MDF. Copula functions can  
116 be expressed as:

$$117 C_{\theta}(u_1, u_2 \dots u_n) = C_{\theta}[F_1(x_1), F_2(x_2) \dots F_n(x_n)] \quad (1)$$

118 where  $x_1, x_2 \dots x_n$  are random vectors,  $F_1(x_1), F_2(x_2) \dots F_n(x_n)$  are MDF of the random vectors,  $\theta$   
119 is the parameter of copula function.

120 Copula functions are mainly classified into Archimedean, elliptic, and quadratic types. Among them,  
121 Archimedean Copula functions have been widely applied in the field of hydrology. The most used  
122 Archimedean Copula multidimensional joint distribution models are the following:

123 (1) GH-Copula joint distribution model

$$124 C_{\theta}(u_1, u_2 \dots u_n) = \exp \left[ -(\sum_{i=1}^n (-\ln u_i)^{\theta})^{\frac{1}{\theta}} \right] \quad (\theta > 1), \quad (2)$$

125 (2) Clayton Copula joint distribution model

$$126 C_{\theta}(u_1, u_2 \dots u_n) = \left[ 1 + \sum_{i=1}^n (u_i^{-\theta} - 1) \right]^{-\frac{1}{\theta}} \quad (\theta > 1), \quad (3)$$

127 (3) Frank Copula joint distribution model

$$128 C_{\theta}(u_1, u_2 \dots u_n) = -\frac{1}{\theta} \ln \left[ 1 + \frac{\prod_{i=1}^n (e^{-\theta u_i} - 1)}{(e^{-\theta} - 1)^{n-1}} \right] \quad (\theta > 1), \quad (4)$$

129 The steps of Copula function-based wet-dry encounter analysis are as follows:

- 130 1. Fit the MDF. The widely applied probability distribution functions are mainly Pearson type 3  
131 distribution (P-III), T-distribution, Normal distribution, etc.
- 132 2. Select the MDF. Fitting different MDF of the runoff, using the AIC criterion for the selection of the  
133 fitted MDF.
- 134 3. Fitting Copula distribution function.

### 135 3.2 Method of CM-ROPAR

136 The CM-ROPAR algorithm consists of the four main parts. The first part is to generate scenarios of  
137 drought-wet encounters. The second part is to sample and generate the Pareto front. In this part, the  
138 uncertain parameters are sampled firstly. Then a MOO is performed for each sample to generate a Pareto  
139 front. The number of Pareto fronts is equal to the number of samples sampled. The third part is a  
140 probabilistic analysis of the Pareto front set. The last part is to identify the robust solution. The specific  
141 process of optimal water allocation under runoff uncertainty based on CM-ROPAR algorithm is as  
142 follows.

143 **Part I** (Analyzing the wet-dry encounters)

- 144 1. Analyze the inflow wet and dry encounters. If the basin has  $k$  inflows, then there are  $3^k$  wet-dry  
145 scenarios. For example, suppose there is one inflow in the upper and one in the middle reaches of the  
146 basin. In that case, there are 9 scenarios: wet-medium, wet-wet, medium-wet, medium-medium, medium-  
147 dry, dry-wet, dry-medium, and dry-dry.
- 148 2. Choose a scenario from 1 to  $3^k$ .



149 **Part 2** (Sampling-Inflow)

150 3. Based on the recorded annual inflow data  $Q$ , it is assumed that  $Q$  is not a definite value but

151  $Q = i_{uncertainty} * Q,$  (5)

152  $i_{uncertainty} \sim N(1, 0.0025),$  (6)

153 where  $i_{uncertainty}$  follows a normal distribution with a mean of 1 and a standard deviation of 0.05.

154 4. For  $i = 1, 2, \dots, np$  do

155 5. Sample  $u$  (inflow). As mentioned before, the uncertainty variable is obtained from the normal  
156 distribution  $N(1, 0.0025)$ . This represents that a 99.74% probability of the uncertainty variable falling  
157 within the interval  $[0.85, 1.15]$  and the inflow sample falling within the interval  $[0.85 * Q, 1.15 * Q]$ .

158 6. Find the Pareto front  $F_r$  by solving the deterministic multi-objective optimization problem for sample  
159  $u_r$ .

160 **Part 3** (Forming the optimal solution set through  $np$  Pareto fronts)

161 7. Select an ideal solution ( $IS$ ) in each Pareto front  $F_r$  based on the distance to the origin point, forming  
162 the optimal solution set (set  $S$ ).

163 **Part 4** (Evaluating the robustness of each solution)

164 8. Select a solution  $s_i$  ( $i = 1, \dots, np$ ) from the solution set  $S$ .

165 9. Cast the inflow case  $u_r$  ( $r = 1, \dots, np$ ) into  $s_i$  and calculate  $P_r(u_r, s_i)$  and  $WD_r(u_r, s_i)$ ,  
166 respectively, to form 1200 values of  $P_r$  and  $WD_r$  ( $r = 1, \dots, np$ ).

167 10. Select the robustness evaluation criteria,  $RC1, RC2, RC3, RC4$ .

168 11. For each  $s_i$  ( $i = 1, 2, \dots, np$ ), calculate the  $RC1, RC2, RC3, RC4$  and  $SRI$  corresponding to  $P_r$  and  
169  $WD_r$  respectively. Plot the corresponding graphs and find the Pareto front of each graph.

170 12. Find the solution with the highest robustness.

171 End

172 3.3 Defining the robustness criteria

173 According to the general definition of robustness, four common Robustness Criteria ( $RC$ ) were used in  
174 this study (Beyer and Sendhoff, 2007). These must be minimized to achieve the maximum robustness of  
175 the solution, so the lower the criteria, the higher the robustness.

176 For the four  $RC$ , two MOO are implicitly defined, and optimization can be named Two Layer-Multi-  
177 objective optimization of Robustness Criteria (TL-MOORC). It is worth noting that TL-MOORC differs  
178 from the problem's MOO. A one-layer MOORC is a solution that may not be minimized at all four  $RC$   
179 simultaneously. This problem can be solved by aggregating the four  $RC$  into one, for example, using a  
180 linear weighted combination. The second layer of MOORC is that for the two objective functions of a  
181 solution, the  $RC$  for both objective functions may not be minimized at the same time. Therefore, a trade-  
182 off must be made between the  $RC$  for the two objective functions.

183 The first  $RC$  is the expected value of each objective function, denoted as  $RC1$ . It reflects the fact that  
184 we want to find a solution that is good on average across all uncertainties and can be represented by:

185  $RC1(s) = \int_{N(s,u)} f(s, u) p(u) du,$  (7)

186 where  $p(u)$  is the probability density function of the uncertain variable  $u$ ; it is the neighborhood of the  
187 solution  $s$ .

188 The second  $RC$  is the 'worst case' (or 'minimax' case), denoted as  $RC2$ . This  $RC$  is related to  
189 robustness because we want to find a solution  $s$  such that the value of each objective function in the  
190 worst case is the minimum possible. It can be presented as follows:



191  $RC2(s) = \min \left( \max_{N(s,u)} (f(s,u)) \right),$  (8)

192 The third *RC* is the ‘standard deviation’ of each objective function, denoted as *RC3*. *RC3* is  
 193 related to the robustness of each objective function because we want to find a solution *s* such that the  
 194 value of the objective function would not vary too much due to uncertainty. It can be expressed as follows:

195  $RC3(s) = \sqrt{\int_{N(s,u)} (f(s,u) - f(u))^2 p(u) du},$  (9)

196 The fourth *RC* is the "probabilistic threshold", denoted as *RC4*. We want to find a solution *s* that  
 197 minimizes the probability that the objective function is higher than the threshold of interest *q*. This  
 198 criterion is usually associated with the reliability of the system. It can be expressed as follows:

199  $RC4(s) = Pr(f(s,u) > q|s),$  (10)

200 In order to evaluate the integrated robustness of the water resources allocation scheme, the weighted sum  
 201 of the four Normalized *RC* (*NRCi*) in this study was used as the integrated robustness criteria. In this  
 202 study, we consider that the four *RC* to be of equal importance, so all four indicators are given a weight  
 203 of  $\frac{1}{4}$ .

204  $SRI = \frac{1}{4}NRC1 + \frac{1}{4}NRC2 + \frac{1}{4}NRC3 + \frac{1}{4}NRC4,$  (11)

205 (of course, other ways of aggregation can be considered as well.)

206 3.4 Construction of WRA Model

207 Objective function

208 (1) Social Goals: Water Deficit (*WD*)

209  $min f_1(Q) = \sum_{j=1}^J \sum_{k=1}^K \left( \frac{D_{jk} - \sum_{t=1}^T \sum_{i=1}^I Q_{ijkt}}{D_{jk}} \right)^2,$  (12)

210 Where  $D_{jk}$  denotes the water demand of the water consumption department *k* of the city *j*.  $Q_{ijkt}$  is the  
 211 water supply quantity of water source *i* to water consumption department *k* of the city *j* in the period  
 212 *t*.

213 (2) Ecological goals: Pollution (*P*)

214  $min f_2(Q) = \sum_{j=1}^J \sum_{k=1}^K d_{jk} p_{jk} \sum_{i=1}^I \sum_{t=1}^T Q_{ijkt},$  (13)

215 Where  $d_{jk}$  denotes the representative pollutant discharge per unit of wastewater of the water department  
 216 *k* of calculation unit *j* ( $ton/m^3$ ) and  $p_{jk}$  represents the sewage discharge coefficient of the water  
 217 consumption department of calculation unit. Discharge coefficient of water consumption department *k*  
 218 of calculation unit *j*.  $Q_{ijkt}$  is the water supply quantity of water source *i* to water consumption  
 219 department of calculation *k* unit *j* in the period *t*.

220 Constraints



221 (1) Water demand constraint  
 222  $\min D_{jk} \leq \sum_{i=1}^I \sum_{t=1}^T Q_{ijkt} \leq \max D_{jk},$  (14)

223 (2) Water supply capacity constraint  
 224  $\sum_{k=1}^K \sum_{j=1}^J \sum_{t=1}^T Q_{ijk} \leq U_i,$  (15)

225 (3) Water Resources Constraint  
 226  $\sum_{j=1}^J \sum_{k=1}^K Q_{ijk} \leq WR_i,$  (16)

227 4. Results and discussion

228 4.1 Identification of marginal distribution functions

229 According to the first part (step 1-2) of the CM-ROPAR process, we need to construct the joint  
 230 probability distributions for the upstream and midstream inflow and generate nine inflow scenarios via  
 231 the Copula function. Therefore, before constructing the JDF, we need to construct the MDF for the  
 232 upstream and midstream inflows respectively. Based on the Kolmogorov-Smirnov (K-S) test results, we  
 233 found that the best-fitting distributions for the upstream and midstream were the Weibull and P-III  
 234 distributions, respectively.

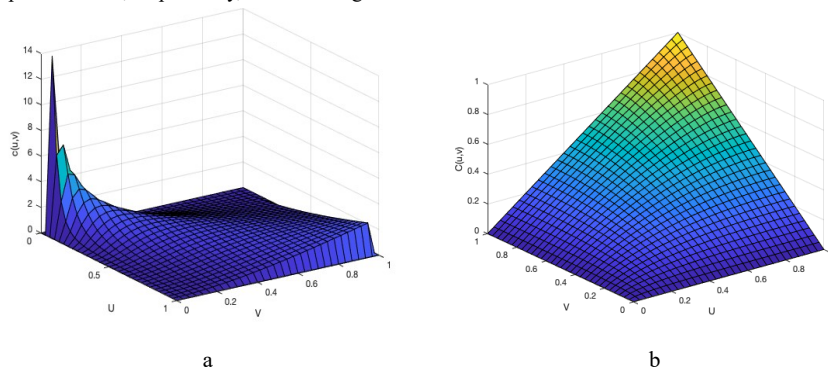
235 4.2 Analysis of upstream and midstream dry and wet encounters

236 The optimal Copula function is selected by comparing the Akaike information criterion (AIC) and the  
 237 Bayesian information criterion (BIC), AIC and BIC values in Table 1. It can be concluded that the joint  
 238 distribution function of the upper and middle reaches of the HRB is consistent with the joint distribution  
 239 of the Clayton Copula function.

240 **Table 1.** AIC and BIC values for Copula functions.

	Gaussian	t	Clayton	Gumbel	Frank
AIC	-20.86	-18.34	<b>-22.69</b>	-12.47	-20.03
BIC	-19.06	-14.73	<b>-20.88</b>	-10.67	-18.22

241 Substituting the multi-year annual inflow for the upper and middle reaches of the HRB into the Clayton  
 242 Copula function, respectively, the following results were obtained.



243 **Figure 4.** Clayton Copula function.

244 As shown in Figure 4, the joint distribution of the annual incoming water in the upper and middle reaches  
 245 of the HRB has symmetry. In addition, the joint distribution of annual water in the upper and middle  
 246 reaches has a tail correlation, which indicates a higher probability of simultaneous wetness or drought in





247 the upper and middle reaches.

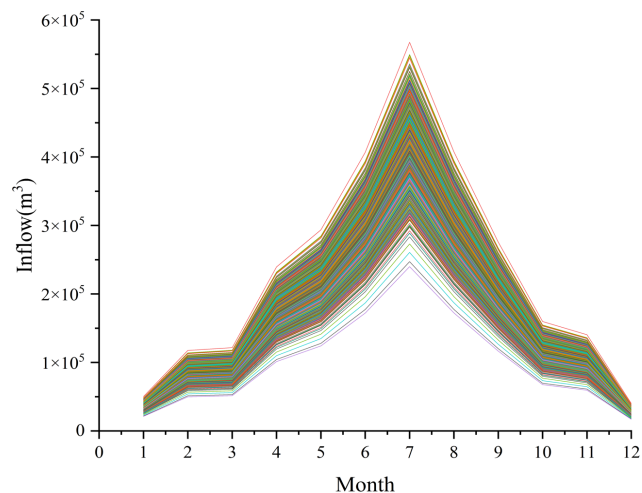
248 **Table 2.** The probabilities of 9 scenarios.

Wet and Dry encounters/%		Upstream		
		Wet	Medium	Dry
Middlestream	Wet	27.7	7.8	5.3
	Medium	11.6	6.5	4.6
	Dry	4.6	7.8	24.1

249 As shown in Table 2, the probability of drought-wetness synchronization in the upper and middle reaches  
 250 of the HRB is 58.3%, while the probability of asynchrony is 41.7%. The former is 16.6% higher than the  
 251 latter, indicating that the upper and middle reaches are less able to complement each other. The joint  
 252 distribution has a maximum probability of 27.7% that the upstream and midstream are both wet, and the  
 253 risk of water scarcity is minimal under this scenario. The joint distribution has the second-highest  
 254 probability of both upstream and midstream being dry at 24.1%, with the highest risk of water scarcity  
 255 under this scenario.

#### 256 4.3 Considering solutions for the uncertainty of inflow through MROPAR

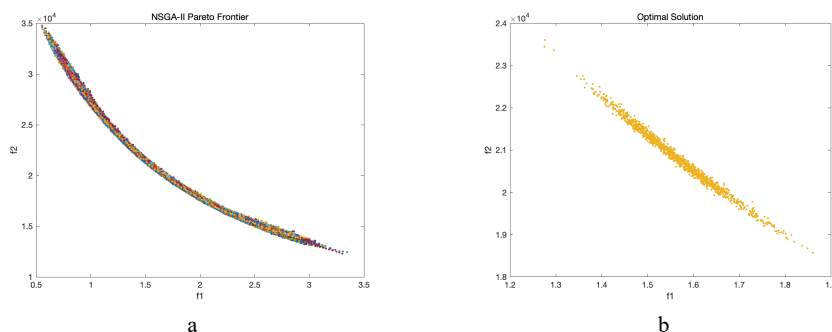
257 In this study the situation when the upper and middle reaches are both wet is considered as a case study.  
 258 For deterministic optimization we opted for the NSGA-II algorithm, which is widely used and has good  
 259 historical performance (Reed et al., 2013). Inflow uncertainty is modelled by sampling 1200 inflows, as  
 260 shown in Figure 5.



261

262 **Figure 5.** Inflow samples.

263 Figure 6(a) shows that 1200 Pareto fronts calculated for each sampled inflow, through steps 3-6 of CM-  
 264 ROPAR. Figure 6(b) shows 1200 ideal solutions  $S$ , selected based on their distance to the ideal solution  
 265 (step 7 of CM-ROPAR).



266 **Figure 6.** a: 1200 Pareto fronts (f1: water deficit; f2: pollution) and b: 1200 ideal solutions (f1: water  
 267 deficit; f2: pollution) selected based on their distance to the ideal solution.

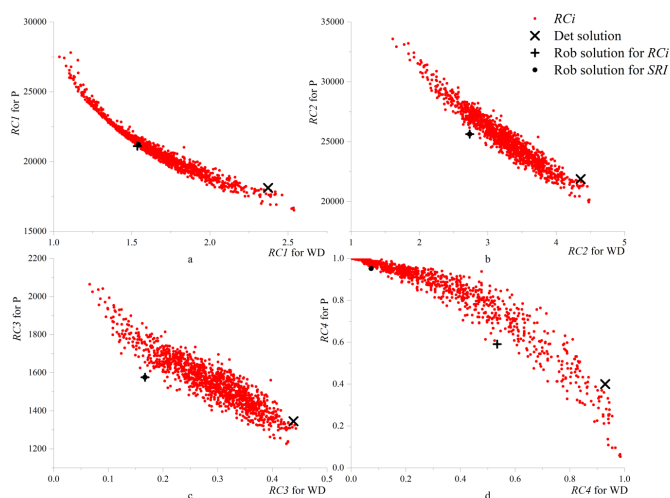
268 **4.4 Assessing robustness of the solutions found by CM-ROPAR**

269 Four robustness criteria are calculated for each solution  $s$  in the solution set  $S$ . Given the solution  $s$   
 270 to be evaluated, it is necessary to calculate  $WD(s, IF_r)(r = 1, \dots, np)$  and  $P(s, IF_r)(r = 1, \dots, np)$  in  
 271 order to calculate the four robustness criteria, where  $IF_r$  is the  $r$ th sample of inflow.  $r$  depends on  
 272 the number of samples; in this study, 1200 samples were taken, so  $np$  is 1200.

273 As shown in Table 3 and Figure 7,  $RC1, RC2, RC3, RC4$  and  $SRI$  for  $WD$  and  $P$  can be calculated  
 274 for each solution in  $S$ , and the solutions corresponding to the smallest value in each  $RCi$  and the  
 275 solutions corresponding to the smallest value in  $SRI$  can be identified, respectively. In addition, we also  
 276 feed 1200 samples to the deterministic solution and calculate  $RC1, RC2, RC3, RC4$  and  $SRI$  for  $WD$   
 277 and  $P$ .

278 **Table 3.** Optimal solution numbers for different robustness criteria.

	$RC1$	$RC2$	$RC3$	$RC4$	$SRI$
$WD$	535	361	361	361	361
$P$	876	876	876	876	876
$IS$	629	84	84	915	84



279  
280 **Figure 7.** Performance of the robustness of solutions (a:  $RC1$ , b:  $RC2$ , c:  $RC3$ , d:  $RC4$ ): robust model  
281 solutions (red dots), deterministic model solution (black  $\times$ ), solution closest to origin for  $RCi$  (black +),  
282 solution closest to origin for  $SRI$  (black dot). The horizontal axis represents the performance of the  
283 robustness for  $WD$ . The vertical axis represents the robustness performance for  $P$ .

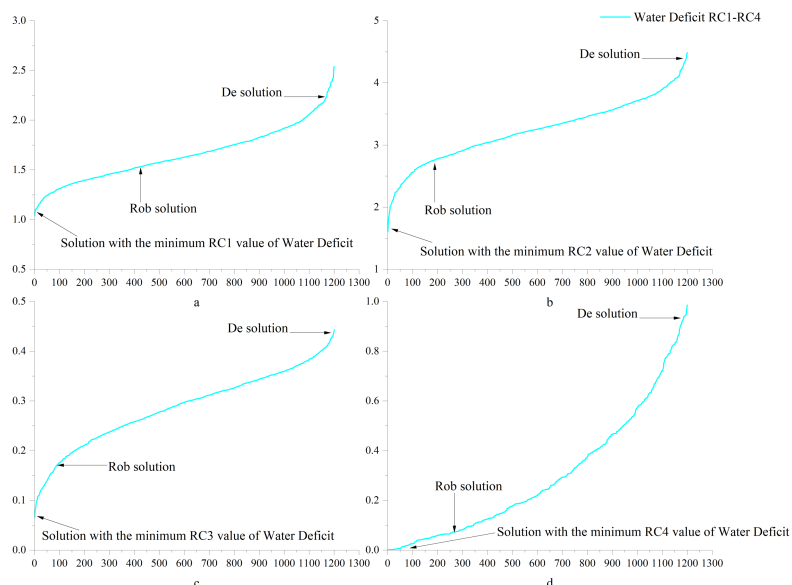
284  
285 Figure 7 shows the performance of 1200 robust model solutions (red dots) and one deterministic model  
286 solution (black  $\times$ ), for the four robustness criteria. From Figure 7, four Pareto fronts can also be found,  
287 which indicate the competitive relationship between water deficit and pollution emissions for each  
288 robustness criterion dimension. As shown in Figure 7(a), we can observe an interesting phenomenon that  
289 the left-most extreme solution (red dot) has the smallest robustness index  $RC1$  for water deficit, but the  
290 highest robustness index  $RC1$  for pollution; the right-most extreme solution (red dot) has the largest  
291 robustness index  $RC1$  for water deficit, but the smallest robustness index  $RC1$  for pollution. Similarly,  
292 this phenomenon can be also observed for the robustness criteria  $RC2$ ,  $RC3$ , and  $RC4$ . More  
293 importantly, as shown in Table 3, the extreme solutions and the solutions closest to the origin point may  
294 differ for different robustness criteria. Specifically, for  $RC1$ , solution No. 535 is the most robust for  
295 water deficit, and solution No. 876 is the most robust for pollution; for  $RC2$ ,  $RC3$ , and  $RC4$ , the most  
296 robust solution for water deficit is solution No. 361, and the most robust solution for pollution is solution  
297 No. 876.

298 Because there are many non-inferior solutions in the Pareto frontier, the decision-makers must choose  
299 among them. The decision-makers need not only to choose among the non-inferior solutions but also to  
300 evaluate the trade-off between different robustness criteria or to choose the best one by combining the  
301 criteria. This study takes the distance to the origin as the basis for such choice. As shown in Table 3, for  
302  $RC1$ ,  $RC2$ ,  $RC3$ , and  $RC4$ , the closest points to the origin are solution No. 629, solution No. 84, and  
303 solution No. 915, respectively.

#### 304 4.5 Comparing solutions found by deterministic and robust approaches

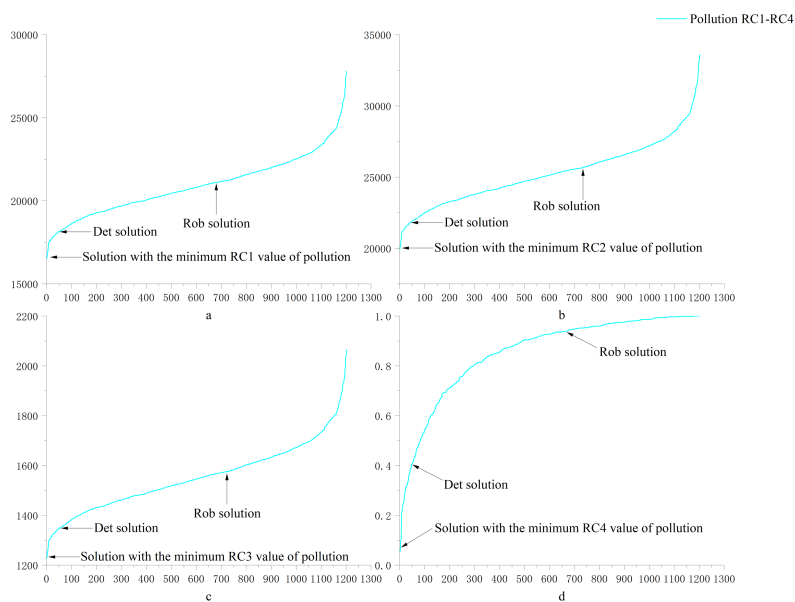


305 To see a more general relationship between the 1201 solutions (i.e., 1200 from the robust optimization  
306 solution and 1 from the deterministic optimization solution), the performance of each solution for water  
307 deficit and pollution on each of the four robustness criteria is plotted in Figure 8 and Figure 9.



308  
309 **Figure 8.** Robustness of water deficit (a:  $RC1$ , b:  $RC2$ , c:  $RC3$ , d:  $RC4$ ).

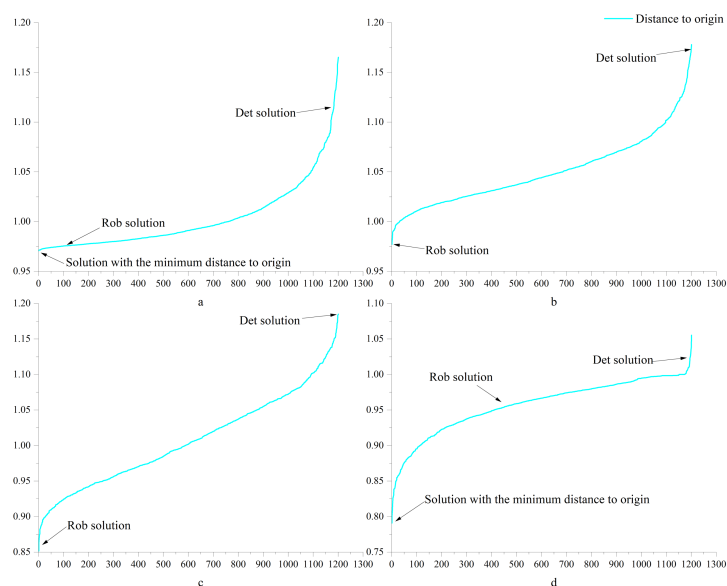
310 As shown in Figure 8, for water scarcity, the robust solution performed significantly better than the  
311 deterministic solution. Specifically, for the four robustness criteria, the robust solution outperforms  
312 63.1%, 85.6%, 92.7%, and 77.7% of the solutions, respectively, while the deterministic solution  
313 outperforms only approximately 1% of the solutions. To analyze the robust and deterministic solutions  
314 more accurately and intuitively, this study applied the ratio of  $RC(Det)/RC(Rob)$  to compare the  
315 robustness of the two solutions. The ratios of  $RC(Det)/RC(Rob)$  are 1.53, 1.59, 2.62, and 12.67 in the  
316 four robustness criteria dimensions. This means that, regarding water deficit, the deterministic model  
317 solution may lead to 53%, 59%, 162%, and 1167% more variability in the four robustness criteria  
318 dimensions.



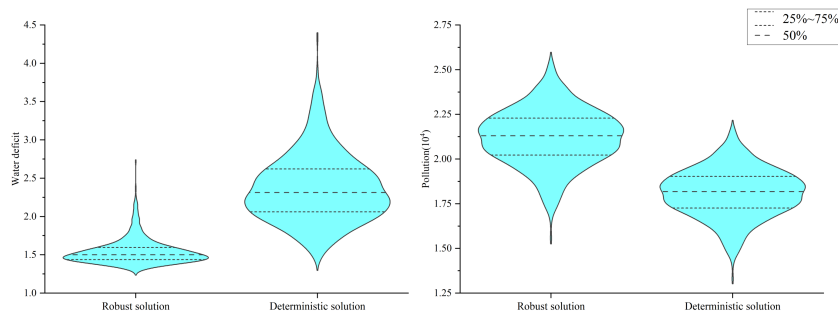
319

320 **Figure 9.** Robustness of pollution (a:  $RC1$ , b:  $RC2$ , c:  $RC3$ , d:  $RC4$ ).

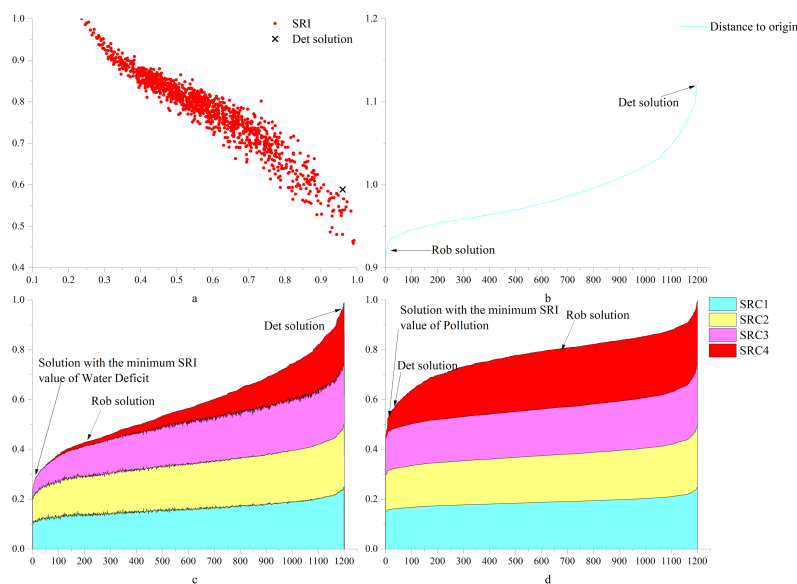
321 However, as shown in Figure 9, the deterministic solution slightly outperforms the robust solution for  
322 pollution. Specifically, for the four robustness criteria, the deterministic solution outperforms 96% of the  
323 solutions, respectively, while the robust solution outperforms about 40% of the solutions. Similarly, we  
324 compare the two solutions by the ratio of  $RC(Rob)/RC(Det)$ . We find that the  $RC(Rob)/RC(Det)$   
325 ratio is about 1.17 for  $RC1$  to  $RC3$  and 2.37 for  $RC4$ . This means that, in terms of pollution, the robust  
326 solution may lead to 17% more variability for  $RC1$  to  $RC3$  and 137% more variability for  $RC4$ .



327  
 328 **Figure 10.** Comprehensive robustness for four indicators (a: *RC1*, b: *RC2*, c: *RC3*, d: *RC4*).  
 329 In order to analyze the comprehensive performance of each solution, rather than just the robustness of a  
 330 single objective, this study reflects the comprehensive implementation of each solution in terms of the  
 331 distance from the solution to the origin. As shown in Figure 10, the comprehensive performance of the  
 332 robust solution for *RC1* to *RC4* is significantly better than that of the deterministic model solution.  
 333 Specifically, the robust solution outperforms 90.3% and 62.2% of the solutions in *RC1* and *RC4*,  
 334 respectively, and outperforms all solutions in *RC2* and *RC3*, while the deterministic solution performs  
 335 exceptionally poorly in all four robustness criteria. According to the ratio of  $Dis(Rob)/Dis(Det)$ , we  
 336 can find that the robust solution is 16.8%, 19.8%, 39.2%, and 7.3% more robust than the deterministic  
 337 solution in the four robustness dimensions, respectively.



338  
 339 **Figure 11.** The integrated robustness index distribution of the robust and deterministic solution.



340  
 341 **Figure 12.** Comprehensive robustness criteria performance (a: Performance of comprehensive  
 342 robustness criterion, b: Comprehensive robustness of robust solutions and deterministic solution, c and  
 343 d: comprehensive robustness criteria for water deficit and pollution).

344 As shown in Figure 11, for water scarcity, the integrated criteria of the robust solution is clustered at  
 345 approximately 0.5 and is significantly more robust than the deterministic solution; for pollution, the  
 346 integrated index of the robust solution is significantly higher than that of the deterministic solution, but  
 347 the span of the integrated index of the two solutions is similar, so the robustness of the deterministic  
 348 solution is slightly better than that of the robust solution.

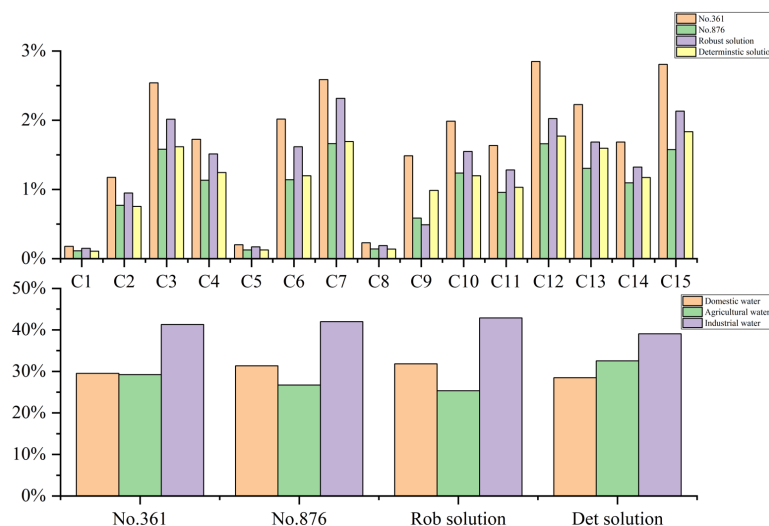
349 Similarly, as shown in Figure 12, there is also a Pareto front for the composite robustness criteria. For  
 350 water deficit, the robustness of the robust solution is better than the deterministic solution; for pollution,  
 351 the robustness of the deterministic solution is better than the robust solution. Specifically, for water deficit,  
 352 the robust solution outperforms 85.3% of the solutions while the deterministic solution outperforms only  
 353 about 1% of the solutions; for pollution, the deterministic solution outperforms 96% of the solutions  
 354 while the robust solution outperforms only 39.6% of the solutions. According to the ratio of  
 355  $SRI(Rob)/SRI(Det)$ , the deterministic solution is about 130% more uncertain than the robust solution  
 356 for water deficit; for pollution, the robust solution is about 37.7% more variable than the deterministic  
 357 solution. The distance of each solution to the origin can reflect the comprehensive performance of the  
 358 robustness of each solution. For the robustness composite index, the ratio of  $Dis(Rob)/Dis(Det)$  is  
 359 0.655, which means that the composite robustness of the robust solution is 52.6% higher than the  
 360 robustness of the deterministic solution.

361 For the robustness composite, the robust solution outperforms all the solutions, while the deterministic  
 362 model solution outperforms only about 3.2% of the solutions. Comparing the distance to the origin of  
 363 the robust solution and the deterministic solution, we can find that the robustness of the robust solution  
 364 improves by 27.8% over the deterministic solution.

#### 365 4.6 Analysis of specific water resources allocation schemes



366 First, as shown in Figure 13, we analyzed the proportion of water supply for each city. We find that the  
 367 water supply share for the scheme most robust to water deficit rates is significantly higher than that for  
 368 the scheme with the most robust pollutant emissions. This is because an increase in water supply leads  
 369 to an increase in pollutant emissions, which in turn leads to a decrease in the robustness of pollutant  
 370 emissions. For specific cities, the least robust allocation scenario for water deficit reduces the water  
 371 supply in City 3, City 7, City 10, City 12, and City 15 compared to the most robust allocation scenario  
 372 for pollutant emissions. Interestingly, these cities have the most water demand in the basin (as shown in  
 373 Figure 3). Therefore, basin managers can increase the water supply to these cities if they need to improve  
 374 the water deficit robustness of the water resources allocation scheme.  
 375 Then we analyze specifically the distribution of water resources between sectors. An interesting  
 376 phenomenon can be observed. As shown in Figure 13, although the scenario with the best robustness in  
 377 terms of pollutant emissions has a lower water supply than the scenario with the best robustness in terms  
 378 of water deficit, the reduction is mainly in the agricultural sector. Water for domestic and industrial  
 379 production did not change much. The reason for this may be that agricultural water use causes more  
 380 pollution and may create more uncertainty. So how can watershed managers hope that improving the  
 381 robustness of pollutant discharge can reduce water supply to the agricultural sector.



382  
 383 **Figure 13.** Specific water resources allocation schemes.

384 **5. Conclusion**

385 In this study, we propose a multi-objective robustness analysis method considering multiple uncertainties  
 386 (CM-ROPAR approach) based on the robust optimization method for uncertainty perception (ROPAR  
 387 approach). To verify the superiority and practicality of the CM-ROPAR approach, four robustness criteria  
 388 are selected, and we compare the robust solution calculated by the method with the optimal solution of  
 389 the deterministic model. In the studied case, CM-ROPAR found a more robust solution.  
 390 The CM-ROPAR approach permits to exhibit the handling of uncertainty, to be able to analyze how  
 391 uncertainty is transmitted to the Pareto frontier, and to perform the corresponding probabilistic analysis.  
 392 The novelty of the new method compared to existing ROPAR methods is reflected in two aspects. First,





393 the ROPAR method only considers uncertainty at a single point. In contrast, the CM-ROPAR method  
394 considers multiple uncertainties through the joint probability distribution of two points, which is closer  
395 to the actual situation and more general. Second, the new way analyzes the robustness of two objective  
396 functions of the solution instead of fixing one objective function to analyze the robustness of the other  
397 objective function. The CM-ROPAR method is more comprehensive and can identify the robustness of  
398 both objective functions, giving decision-makers more information for decision making.  
399 One of the limitations of this study is that the CM-ROPAR approach is applicable to problems with two  
400 uncertainties and two objective functions; however, water allocation allows for more uncertainties and  
401 more objective functions (e.g., the uncertainty of inflow between multiple tributaries). In future research,  
402 we will focus on more complex objective functions and multi-objective optimization problems with at  
403 least three objective functions.

404

405 *Author contribution.* JZ and DS conceptualized the study and wrote the paper. ZD provided the data. All  
406 the authors took part in the interpretation of the results and edits of the paper.

407

408 *Competing interests.* The authors declare that they have no conflict of interest. Dimitri Solomatine is one  
409 of a member of the editorial board of Hydrology and Earth System Sciences.

410

411 *Acknowledgements.* This research has been supported by the projects: Study on the layout of the water  
412 network in Hunan Province (No. XSKJ2021000-05) and Research and application of key technologies  
413 for water resources deployment in the water network system of the Quanmutang Reservoir.

414

415 *Data availability.* The code and computed data are available upon request to the corresponding author.

416

## 417 **Reference**

418 Abdulkaki, D., Al-Hindi, M., Yassine, A., and Abou Najm, M.: An optimization model for the allocation  
419 of water resources, *Journal of Cleaner Production*, 164, 994-1006, 10.1016/j.jclepro.2017.07.024, 2017.

420 Ashofteh, P. S., Haddad, O. B., and A. Mariño, M.: Climate Change Impact on Reservoir Performance  
421 Indexes in Agricultural Water Supply, *Journal of Irrigation and Drainage Engineering*, 139, 85-97,  
422 10.1061/(asce)ir.1943-4774.0000496, 2013.

423 Beyer, H.-G. and Sendhoff, B.: Robust optimization – A comprehensive survey, *Computer Methods in  
424 Applied Mechanics and Engineering*, 196, 3190-3218, 10.1016/j.cma.2007.03.003, 2007.

425 Chen, L., Xu, L., and Yang, Z.: Accounting carbon emission changes under regional industrial transfer  
426 in an urban agglomeration in China's Pearl River Delta, *Journal of Cleaner Production*, 167, 110-119,  
427 10.1016/j.jclepro.2017.08.041, 2017.

428 Dong, Y. and Xu, L.: Aggregate risk of reactive nitrogen under anthropogenic disturbance in the Pearl  
429 River Delta urban agglomeration, *Journal of Cleaner Production*, 211, 490-502,  
430 10.1016/j.jclepro.2018.11.194, 2019.

431 Habibi Davijani, M., Banihabib, M. E., Nadjafzadeh Anvar, A., and Hashemi, S. R.: Multi-Objective  
432 Optimization Model for the Allocation of Water Resources in Arid Regions Based on the Maximization  
433 of Socioeconomic Efficiency, *Water Resources Management*, 30, 927-946, 10.1007/s11269-015-1200-y,  
434 2016.

435 Hassanzadeh, E., Elshorbagy, A., Wheeler, H., and Gober, P.: A risk-based framework for water resource  
436 management under changing water availability, policy options, and irrigation expansion, *Advances in*



- 437 Water Resources, 94, 291-306, 10.1016/j.advwatres.2016.05.018, 2016.
- 438 Jin, S. W., Li, Y. P., Yu, L., Suo, C., and Zhang, K.: Multidivisional planning model for energy, water and  
439 environment considering synergies, trade-offs and uncertainty, *Journal of Cleaner Production*, 259,  
440 10.1016/j.jclepro.2020.121070, 2020.
- 441 Kang, D. and Lansey, K.: Scenario-Based Robust Optimization of Regional Water and Wastewater  
442 Infrastructure, *Journal of Water Resources Planning and Management*, 139, 325-338,  
443 10.1061/(asce)wr.1943-5452.0000236, 2013.
- 444 Kapelan, Z., Savic, D. A., Walters, G. A., and Babayan, A. V.: Risk- and robustness-based solutions to a  
445 multi-objective water distribution system rehabilitation problem under uncertainty, *Water Sci Technol*,  
446 53, 61-75, 10.2166/wst.2006.008, 2006.
- 447 Kapelan, Z. S., Savic, D. A., and Walters, G. A.: Multiobjective design of water distribution systems  
448 under uncertainty, *Water Resources Research*, 41, 10.1029/2004wr003787, 2005.
- 449 Keath, N. A. and Brown, R. R.: Extreme events: being prepared for the pitfalls with progressing  
450 sustainable urban water management, *Water Sci Technol*, 59, 1271-1280, 10.2166/wst.2009.136, 2009.
- 451 Li, M., Fu, Q., Singh, V. P., Liu, D., and Gong, X.: Risk-based agricultural water allocation under multiple  
452 uncertainties, *Agricultural Water Management*, 233, 10.1016/j.agwat.2020.106105, 2020.
- 453 Lu, H., Ren, L., Chen, Y., Tian, P., and Liu, J.: A cloud model based multi-attribute decision making  
454 approach for selection and evaluation of groundwater management schemes, *Journal of Hydrology*, 555,  
455 881-893, 10.1016/j.jhydrol.2017.10.009, 2017.
- 456 Ma, Y., Li, Y. P., and Huang, G. H.: A bi-level chance-constrained programming method for quantifying  
457 the effectiveness of water-trading to water-food-ecology nexus in Amu Darya River basin of Central Asia,  
458 *Environ Res*, 183, 109229, 10.1016/j.envres.2020.109229, 2020.
- 459 Marchi, A., Dandy, G. C., and Maier, H. R.: Integrated Approach for Optimizing the Design of Aquifer  
460 Storage and Recovery Stormwater Harvesting Schemes Accounting for Externalities and Climate Change,  
461 *Journal of Water Resources Planning and Management*, 142, 10.1061/(asce)wr.1943-5452.0000628,  
462 2016.
- 463 Marquez Calvo, O. O., Quintiliani, C., Alfonso, L., Di Cristo, C., Leopardi, A., Solomatine, D., and de  
464 Marinis, G.: Robust optimization of valve management to improve water quality in WDNs under demand  
465 uncertainty, *Urban Water Journal*, 15, 943-952, 10.1080/1573062x.2019.1595673, 2019.
- 466 Nelsen, R. B., Quesada-Molina, J. J., Rodríguez-Lallena, J. A., and Úbeda-Flores, M.: On the  
467 construction of copulas and quasi-copulas with given diagonal sections, *Insurance: Mathematics and  
468 Economics*, 42, 473-483, 10.1016/j.insmatheco.2006.11.011, 2008.
- 469 Nikoo, M. R., Kerachian, R., Karimi, A., and Azadnia, A. A.: Optimal water and waste-load allocations  
470 in rivers using a fuzzy transformation technique: a case study, *Environ Monit Assess*, 185, 2483-2502,  
471 10.1007/s10661-012-2726-6, 2013.
- 472 Quintiliani, C., Marquez-Calvo, O., Alfonso, L., Di Cristo, C., Leopardi, A., Solomatine, D. P., and de  
473 Marinis, G.: Multiobjective Valve Management Optimization Formulations for Water Quality  
474 Enhancement in Water Distribution Networks, *Journal of Water Resources Planning and Management*,  
475 145, 10.1061/(asce)wr.1943-5452.0001133, 2019.
- 476 Reed, P. M., Hadka, D., Herman, J. D., Kasprzyk, J. R., and Kollat, J. B.: Evolutionary multiobjective  
477 optimization in water resources: The past, present, and future, *Advances in Water Resources*, 51, 438-  
478 456, 10.1016/j.advwatres.2012.01.005, 2013.
- 479 Ren, C., Li, Z., and Zhang, H.: Integrated multi-objective stochastic fuzzy programming and AHP  
480 method for agricultural water and land optimization allocation under multiple uncertainties, *Journal of*



- 481 Cleaner Production, 210, 12-24, 10.1016/j.jclepro.2018.10.348, 2019.
- 482 Solomatine, D.: An approach to multi-objective robust optimization allowing for explicit analysis of  
483 robustness, <https://www.un-ihe.org/sites/default/files/solomatine-ropar.pdf>, 2012.
- 484 Solomatine, D. P. and Marquez-Calvo, O. O.: Approach to robust multi-objective optimization and  
485 probabilistic analysis: the ROPAR algorithm, Journal of Hydroinformatics, 21, 427-440,  
486 10.2166/hydro.2019.095, 2019.
- 487 Sun, S., Fu, G., Bao, C., and Fang, C.: Identifying hydro-climatic and socioeconomic forces of water  
488 scarcity through structural decomposition analysis: A case study of Beijing city, Sci Total Environ, 687,  
489 590-600, 10.1016/j.scitotenv.2019.06.143, 2019.
- 490 Xiong, W., Li, Y., Pfister, S., Zhang, W., Wang, C., and Wang, P.: Improving water ecosystem  
491 sustainability of urban water system by management strategies optimization, J Environ Manage, 254,  
492 109766, 10.1016/j.jenvman.2019.109766, 2020.
- 493 Xu, Z., Pan, B., Han, M., Zhu, J., and Tian, L.: Spatial-temporal distribution of rainfall erosivity, erosivity  
494 density and correlation with El Niño–Southern Oscillation in the Huaihe River Basin, China, Ecological  
495 Informatics, 52, 14-25, 10.1016/j.ecoinf.2019.04.004, 2019.
- 496 Yang, W., Li, X., Sun, T., Pei, J., and Li, M.: Macrobenthos functional groups as indicators of ecological  
497 restoration in the northern part of China’s Yellow River Delta Wetlands, Ecological Indicators, 82, 381-  
498 391, 10.1016/j.ecolind.2017.06.057, 2017.
- 499 Yazdi, J., Lee, E. H., and Kim, J. H.: Stochastic Multiobjective Optimization Model for Urban Drainage  
500 Network Rehabilitation, Journal of Water Resources Planning and Management, 141,  
501 10.1061/(asce)wr.1943-5452.0000491, 2015.
- 502 Yu, S. and Lu, H.: An integrated model of water resources optimization allocation based on projection  
503 pursuit model – Grey wolf optimization method in a transboundary river basin, Journal of Hydrology,  
504 559, 156-165, 10.1016/j.jhydrol.2018.02.033, 2018.
- 505 Zeng, X., Zhao, J., Wang, D., Kong, X., Zhu, Y., Liu, Z., Dai, W., and Huang, G.: Scenario analysis of a  
506 sustainable water-food nexus optimization with consideration of population-economy regulation in  
507 Beijing-Tianjin-Hebei region, Journal of Cleaner Production, 228, 927-940,  
508 10.1016/j.jclepro.2019.04.319, 2019.
- 509 Zhu, F., Zhong, P.-a., Cao, Q., Chen, J., Sun, Y., and Fu, J.: A stochastic multi-criteria decision making  
510 framework for robust water resources management under uncertainty, Journal of Hydrology, 576, 287-  
511 298, 10.1016/j.jhydrol.2019.06.049, 2019.
- 512 Zhuang, X. W., Li, Y. P., Nie, S., Fan, Y. R., and Huang, G. H.: Analyzing climate change impacts on  
513 water resources under uncertainty using an integrated simulation-optimization approach, Journal of  
514 Hydrology, 556, 523-538, 10.1016/j.jhydrol.2017.11.016, 2018.
- 515